Towards a Universal Veering Profile for Turbulent Ekman Flow at arbitrary Reynolds number - Part 2

LES and DNS of Turbulent Ekman Flow

hauke-zrick

Draft September 14, 2021

Abstract

An analytical formulation for the profiles of stream- and span-wise velocity in turbulent Ekman flow and large-eddy simulations ~~are~~ used to analyze the properties of ~~the~~ turbulent Ekman flow. We show a comparison of a turbulent Ekman flow of $Re_D = 1\,600$ simulated by DNS and LES.

1 Introduction

~~We here consider the~~ turbulent Ekman flow a homogeneous, stationary boundary layer flow over a rotating flat surface under neutral stratification.

~~This flow is defined by only very few parameters. Nevertheless,~~ it can serve as a simple model of the atmospheric boundary layer since it exhibits ~~many~~ characteristics ~~that also shape~~ the real atmosphere ~~namely~~ the logarithmic layer and the Ekman spiral. Hence, the investigation of this case is suited to learn about the fundamental properties of the atmospheric boundary layer.

We investigate three different Reynolds numbers Re_D: 1 600, 150 000, and 1 000 000, where $Re_D = GD/\nu$ and $D = \sqrt{2\nu/f}$, $Re_D = G/\sqrt{\frac{1}{2}\nu f}$. All cases are simulated by LES and the low Reynolds number case we also simulate by DNS for comparison. ~~The too high Reynolds number cases cannot be simulated by DNS due to the limitations of computational resources.~~

Short summary of part I? In part I of this publication, we presented a generic profile of wind direction and speed in turbulent Ekman flow.

The information how the wind direction changes with height is of great importance for wind-power forecasting Optis et al. [2014].

[Wie ist die Grenzschicht? Was sagen die Profile und das LES darüber?]

Foundations: Csanady [1967], Tennekes [1973], Spalart [1989]

Neutral Ekman layer with LES: Esau [2004]Jiang et al. [2018]

The same turbulent Ekman flow is simulated by DNS and LES and the results are compared.

Profile of wind direction from DNS - what can be learned from it for LES?

Limits of coarse resolution

The velocity profiles of both horizontal components of the turbulent Ekman flow provide a benchmark test for LES model. → First step towards a generic wind profile including stratification (and inversion?)?

This paper investigates the mean velocity profiles of the turbulent Ekman flow from moderate to high Reynolds numbers using the formulation from part I and LES.

2 A Universal Velocity Profile for the Turbulent Ekman Layer

The universal velocity profile for the turbulent Ekman layer consists of several parts for different layers of the boundary layer. Near the surface, viscous forces dominate the flow. In the middle

Summary of Comments on manuscript_20210922_CA.pdf .pdf

Page: 1

Number: 1 Author: zrick Subject: Cross-Out Date: 28.09.21, 12:03:52

Number: 2 Author: zrick Subject: Cross-Out Date: 28.09.21, 12:04:00

Number: 3 Author: zrick Subject: Inserted Text Date: 28.09.21, 12:03:54
is

Number: 4 Author: zrick Subject: Cross-Out Date: 28.09.21, 12:04:56

Number: 5 Author: zrick Subject: Cross-Out Date: 28.09.21, 12:04:33

Number: 6 Author: zrick Subject: Cross-Out Date: 28.09.21, 12:05:01

Number: 7 Author: zrick Subject: Inserted Text Date: 28.09.21, 12:05:03
i

Number: 8 Author: zrick Subject: Inserted Text Date: 28.09.21, 12:04:49
horizontally

Number: 9 Author: zrick Subject: Inserted Text Date: 28.09.21, 12:05:58
[no paragraph break befor] Despite its conceptual simplicity,

Number: 10 Author: zrick Subject: Inserted Text Date: 28.09.21, 12:06:45
key

Number: 11 Author: zrick Subject: Inserted Text Date: 28.09.21, 12:06:53
shaping

Number: 12 Author: zrick Subject: Cross-Out Date: 28.09.21, 12:06:59

Number: 13 Author: zrick Subject: Cross-Out Date: 28.09.21, 12:06:58

Number: 14 Author: zrick Subject: Inserted Text Date: 28.09.21, 12:06:58
:

Number: 15 Author: zrick Subject: Sticky Note Date: 28.09.21, 12:07:54
Before talking about the Reynolds number, it would be useful to introduce the concept of scale separation and briefly discuss it with respect to LES.

Number: 16 Author: zrick Subject: Highlight Date: 28.09.21, 12:13:26
While the low-Re case (Re_D=1600) is also investigated by DNS (cf. part 1 of this study), $Re_D=10^6$ corresponds to the scale separation found in typical atmospheric boundary layers. This approach raises our confidence in the LES results to a new level for the direct comparison with a resolving simulation. And it allows us to extend the insight to atmospheric scale where a direct approach is clearly infeasible for computational constraints.

Number: 17 Author: zrick Subject: Cross-Out Date: 28.09.21, 12:13:15

Number: 18 Author: zrick Subject: Sticky Note Date: 28.09.21, 12:14:27
I would avoid this explicitly. The two parts appear together, and part 1 will have abstract, introduction, conclusion, i.e., no reason to duplicate material...

Number: 19 Author: zrick Subject: Highlight Date: 28.09.21, 12:16:27
Should we move this motivation to the very beginning? Maybe with a general sentence introducing the 'increasing relevence of wind power forecasting'..., but not necessarily if we find a better start.

Number: 20 Author: zrick Subject: Sticky Note Date: 28.09.21, 12:17:08
This is very nice idea and important point in placing the work in the context of part 1 and what will follow up.

Number: 21 Author: zrick Subject: Sticky Note Date: 28.09.21, 12:20:03
In a way, this section 2 is previous work. IF we really aim at a most-concise formulation of the profiles, one might think

Comments from page 1 continued on next page

Towards a Universal Veering Profile for Turbulent Ekman Flow at arbitrary Reynolds number - Part 2

LES and DNS of Turbulent Ekman Flow

hauke-zrick

Draft September 14, 2021

Abstract

An analytical formulation for the profiles of stream- and span-wise velocity in turbulent Ekman flow and large-eddy simulations ~~are~~ used to analyze the properties of ~~the~~ turbulent Ekman flow. We show a comparison of a turbulent Ekman flow of $Re_D = 1\,600$ simulated by DNS and LES.

1 Introduction

~~We here consider the~~ turbulent Ekman flow as a homogeneous, stationary boundary layer flow over a rotating flat surface under neutral stratification.

~~This flow is defined by only very few parameters. Nevertheless,~~ it can serve as a simple model of the atmospheric boundary layer since it exhibits ~~many~~ characteristics ~~that also shape~~ the real atmosphere~~, namely~~ the logarithmic layer and the Ekman spiral. Hence, the investigation of this case is suited to learn about the fundamental properties of the atmospheric boundary layer.

We investigate three different Reynolds numbers Re_D: 1 600, 150 000, and 1 000 000, where $Re_D = GD/\nu$ and $D = \sqrt{2\nu/f}$, $Re_D = G/\sqrt{\frac{1}{2}\nu f}$. All cases are simulated by LES and the low Reynolds number case we also simulate by DNS for comparison. ~~The too high Reynolds number cases cannot be simulated by DNS due to the limitations of computational resources.~~

Short summary of part I? In part I of this publication, we presented a generic profile of wind direction and speed in turbulent Ekman flow.

The information how the wind direction changes with height is of great importance for wind-power forecasting Optis et al. [2014].

[Wie ist die Grenzschicht? Was sagen die Profile und das LES darüber?]

Foundations: Csanady [1967], Tennekes [1973], Spalart [1989]

Neutral Ekman layer with LES: Esau [2004]Jiang et al. [2018]

The same turbulent Ekman flow is simulated by DNS and LES and the results are compared.

Profile of wind direction from DNS - what can be learned from it for LES?

Limits of coarse resolution

The velocity profiles of both horizontal components of the turbulent Ekman flow provide a benchmark test for LES model. → First step towards a generic wind profile including stratification (and inversion?)?

This paper investigates the mean velocity profiles of the turbulent Ekman flow from moderate to high Reynolds numbers using the formulation from part I and LES.

2 A Universal Velocity Profile for the Turbulent Ekman Layer

The universal velocity profile for the turbulent Ekman layer consists of several parts for different layers of the boundary layer. Near the surface, viscous forces dominate the flow. In the middle about making this a subsection of section 1 or -- depending on how the manuscript develops -- section 3. In any case, I do not think, it should stand here as a separate section. I therefore do not comment on this section as it appears now.

part, the velocity profile has a logarithmic shape which passes over into an Ekman spiral. In the following, the distinct layers for both horizontal components of the velocity are described.

2.1 Total profile

1 [In part II a summary of the theor. profile in minimalistic form? Without any deductions, just a description.]

From the layers of the velocity profile, a total profile for the whole boundary layer is formed. The profile of the stream-wise component of the velocity is seperated into three layers, which are the viscous layer U_{visc}, the logarithmic layer U_{log}, and the Ekman layer U_{EK}. The span-wise component of the velocity is seperated into two layers, namely the inner layer V_{inner}, and the Ekman layer V_{EK}.

$$U = (1 - w_{visc})U_{visc} + (w_{visc} - w_{outer})U_{log} + w_{outer}U_{EK}, \tag{1}$$
$$V = (1 - w_{outer})V_{inner} + w_{outer}V_{EK}. \tag{2}$$

The transition between consecutive layers is formed by a transfer function:

$$w_* = \frac{1}{2}\left(\mathrm{erf}\left[\sigma_T \log\left(\frac{z}{z_T}\right)\right] + 1\right), \tag{3}$$

where σ_T is a transition scale that defines the width of the transition and z_T is the height of the transition, where the upper and the lower layer equally contribute to the velocity ($w_*(z_T) = 0.5$).

2.2 Drag-Law

The geostrophic drag $Z \equiv u_\star/G$ and the direction between the shear stress and the geostrophic wind α are two key parameters of the Ekman flow. They can be estimated using a semi-empirical drag-law based on Spalart [1989], which describes them as functions of only the Reynolds number:

$$\frac{G}{u_\star}\cos\phi^\star = \frac{1}{\kappa}\log Re_\tau + C - A_r, \tag{4a}$$
$$\sin\phi^\star = A_i\frac{u_\star}{G}, \tag{4b}$$
$$\alpha = \phi^\star - \frac{C_5}{Re_\tau}, \tag{4c}$$

with $Re_\tau = \frac{Re_D^2}{2}\frac{u_\star^2}{G^2}$, $\kappa = 0.415$, $A_r = 4.80$, $A_i = -5.57$, $C = 5.4605$, $C_5 = -57.8$. This law is in excellent agreement with DNS in the range $400 \leq Re_D \leq 1\,600$ as demonstrated by Ansorge and Mellado [2014].

2.3 Stream-wise Velocity Component

In the viscous sublayer, the span-wise velocity is close to zero and the stream-wise velocity is described by the law of the wall:

$$U^{\alpha+} = z^+, \tag{5}$$

(the index α indicates the alignment with the direction of the shear stress). Around $z^+ = 5$, the velocity is beginning to deviate from its linear profile and the buffer layer forms the transition between viscous layer and logarithmic layer. From the surface up to the buffer layer, the stream-wise velocity is described by

$$U^{\alpha+}_{inner} = \frac{z^+ + \gamma_4(z^+)^4 + \gamma_6(z^+)^6}{1 + \gamma_6/u_{ref}(z^+)^6}, \tag{6}$$

Number: 1 Author: zrick Subject: Highlight Date: 28.09.21, 12:19:46

Very good idea!

where $\gamma_4 = -3.825 \cdot 10^{-4}$, $\gamma_6 = 6.32 \cdot 10^{-6}$, and $u_{ref} = 0.07825$.

The logarithmic region of the stream-wise velocity is

$$U_{\log}^{\alpha+} = \frac{1}{\kappa} \log z^+ + C, \tag{7}$$

where $\kappa = 0.416$, and $C = 5.4605$. The transition between buffer layer and logarithmic layer is located at $z_T^+ = 19$ with a scale $\sigma_T = 2$.

2.4 Profile in Outer Layer

Above the boundary layer, the horizontal pressure gradient is balanced by the coriolis force and the wind speed equals the geostrophic wind G. For the stationary case, the horizontal equations of motion can be written

$$0 = fV + \nu_e \partial_z^2 U, \tag{8a}$$

$$0 = -f(U - G) + \nu_e \partial_z^2 V, \tag{8b}$$

where ν_e is an eddy viscosity and the x-axis is aligned with the geostrophic wind. This is solved by

$$U_{EK} = G + Ae^{-\tilde{z}} \cos \tilde{z}, \tag{9a}$$

$$V_{EK} = -Ae^{-\tilde{z}} \sin \tilde{z}, \tag{9b}$$

where $A = 8.4u_\star - 150/Re_\tau$, $\tilde{z} = (z - z_r)/D_E$, $z_r = 0.12\delta$, and $D_E = 3\delta/4\pi \approx 0.24\delta$. The parameters are deduced from DNS.

The transition from the logarithmic layer to the Ekman layer is located at $z^- = 0.3$ (talk: $z_T^- = 0.3 - 120/Re_D$) with a transition scale of $\sigma_T = 2$ for the stream-wise velocity.

2.5 Span-wise Velocity

For $z^+ \leq 10$, the knowledge on U^α is exploited to parametrize V^α in terms of direction:

$$\alpha_{visc} = \frac{C_1 + C_2(\log z^+)^2}{Re_\tau Z}, \tag{10}$$

$$\Rightarrow V_{visc}^\alpha = U^\alpha \tan(\alpha_{visc}), \tag{11}$$

where $C_1 = 40$, $C_2 = 26$, and $Z = u_\star/G$ [(not valid for $z^+ < 1$!?)]. Above $z^+ = 10$, V^α is continued with

$$V_{inner}^\alpha = V_{10}^\alpha + A \log\left(\frac{z^+}{10}\right) + B(z^+ - 10), \tag{12}$$

which matches the value of $V_{10}^\alpha = V_{visc}^\alpha(z^+ = 10)$. To also match the gradient $m_{10} = \partial V_{visc}^\alpha / \partial z^+$ at $z^+ = 10$ and the value of V_{EK}^α at $z^- = 0.27$, the values of A and B need to be

$$A = \frac{V_{EK}^\alpha(z^- = 0.27) - V_{10}^\alpha - m_{10}\,(0.27z^+/Re_\tau - 10)}{\log(0.27z^+/(10Re_\tau)) - (0.27z^+/Re_\tau - 10)/10}, \tag{13}$$

$$B = m_{10} - A/10. \tag{14}$$

At $z_T^- = 0.27$, V_{inner}^α is blended into V_{EK}.

This page contains no comments

Table 1: Key parameters of the simulated cases. f, ν, and G are input parameters, while $u_\star$ and α are the expected results according to Spalart [1989]

Name	Re_D	Re_τ	f [s$^-$1]	ν [m^{2}s$^-$1]	G [ms$^-$1]	$u_\star$ [ms$^-$1]	α [°]
Re1	10^3	$3 \cdot 10^3$	10^{-4}	$1.5 \cdot 10^{-5}$	0.0274	0.00144	18.96
Re2	$1.5 \cdot 10^5$	$7.3 \cdot 10^6$	10^{-4}	$1.5 \cdot 10^{-5}$	4.108	0.1048	8.51
Re3	10^6	$2.2 \cdot 10^8$	10^{-4}	$1.5 \cdot 10^{-5}$	27.39	0.5785	7.03

Table 2: Simulations and grid parameters

Name	Δ [m]	n_x	n_y	n_z	L_x [m]	L_y [m]	L_z [m]
Re1_150	0.14	1536	1536	288	215.04	215.04	123
Re1_150_dyn	0.14	1536	1536	288	215.04	215.04	123
Re1_100	0.2	1080	1080	192	216	216	67.1
Re1_50	0.4	576	576	120	230.4	230.4	77.8
Re2_150	7	1536	1536	288	10752	10752	4245
Re2_100	10	1080	1080	192	10800	10800	3104
Re2_50	20	576	576	120	11520	11520	4113
Re2_l_sq	7	1536	1536	288	10752	10752	4245
Re2_l	7	1536	768	288	10752	5376	4245
Re2_m_sq	7	768	768	288	5376	5376	4245
Re2_m	7	768	384	288	5376	2688	4245
Re2_s	7	384	192	288	2688	1344	4245
Re3_150	40	1536	1536	240	61440	61440	21 600
Re2_150_dyn	7	1536	768	288	10752	5376	4245
Re2_50_dyn	20	576	576	120	11520	11520	4113
Re3_150	40	1536	1536	240	61440	61440	17393
Re3_100	55	1080	1080	192	59400	59400	18687
Re3_50	110	576	576	120	63360	63360	6212

3 Setup

3.1 Settings

An incompressible, turbulent Ekman flow over a flat rotating plate is simulated for three different Reynolds numbers $Re_D = 10^3; 1.5 \cdot 10^5; 10^6$, hereafter $Re1$, $Re2$, and $Re3$, respectively. The key input parameters of the three cases are presented in table 1.

The domain is rotating around the z-axis with an angular velocity such that the Coriolis parameter is $f = 10^{-4}$. The stratification of the flow is ~~entirely~~ neutral, i.e., the potential temperature $\Theta = const.$ for the whole domain. At the upper boundary, a no-penetration boundary condition is used and the horizontal components of the wind are forced to ~~be~~ equal ~~to~~ the geostrophic wind. At the bottom, a constant flux layer is assumed and ~~the~~ Monin-Obukhov theory (MOST) is used to calculate the surface momentum fluxes $\overline{u''w''}_0$ and $\overline{v''w''}_0$.

To study the effect of resolution on the simulations, three different grid resolutions are chosen for each Reynolds number case. The grid cell sizes are around $\delta/50$, $\delta/100$, and $\delta/150$ for a coarse, a medium, and a fine resolution, respectively (see table 2).

The grid spacing inside the boundary layer is isotropic up to the height $\delta = u_\star/f$. ~~From where on the grid spacings in z-direction are stretched with the factor 1.02 each level, up to a maximum grid spacing of $6\Delta x$.~~ The number of vertical grid points is chosen such that ~~the domain height is at least three times~~ δ. Above two thirds of the total domain, Rayleigh damping is active to avoid reflections from the upper boundary.

[The domain-size part rather in the results? Again a mix of setup and presentation of

Page: 4

Number: 1 Author: zrick Subject: Highlight Date: 28.09.21, 15:02:31

These two lines are somehow the same apart from the last number (L_z) --> Does not make sense

Number: 2 Author: zrick Subject: Highlight Date: 28.09.21, 15:02:04

Number: 3 Author: zrick Subject: Highlight Date: 28.09.21, 14:47:18

Case description and numerical set-up

Number: 4 Author: zrick Subject: Cross-Out Date: 28.09.21, 15:03:55

Number: 5 Author: zrick Subject: Inserted Text Date: 28.09.21, 15:03:45

, a value representative of mid-latitude synoptic systems.

Number: 6 Author: zrick Subject: Inserted Text Date: 28.09.21, 15:03:59

truly

Number: 7 Author: zrick Subject: Cross-Out Date: 28.09.21, 15:04:28

Number: 8 Author: zrick Subject: Cross-Out Date: 28.09.21, 15:04:31

Number: 9 Author: zrick Subject: Cross-Out Date: 28.09.21, 15:04:53

Number: 10 Author: zrick Subject: Inserted Text Date: 28.09.21, 15:04:43

through a Dirichlet-type boundary condition

Number: 11 Author: zrick Subject: Highlight Date: 28.09.21, 15:06:36

these quantities have not been defined; you probably need a sub-section introducing either the complete LES (probably not needed), or at least the notation which would go in between 3 and 3.1, i.e. become the new 3.1

Number: 12 Author: zrick Subject: Cross-Out Date: 28.09.21, 15:05:08

Number: 13 Author: zrick Subject: Inserted Text Date: 28.09.21, 15:05:04

similarity t

Number: 14 Author: zrick Subject: Cross-Out Date: 28.09.21, 15:09:22

Number: 15 Author: zrick Subject: Cross-Out Date: 28.09.21, 15:07:24

Number: 16 Author: zrick Subject: Inserted Text Date: 28.09.21, 15:09:07

. Aloft, the grid spacing along Oz is stretched by 2% per grid point until a maximum spacing of $(\Delta z)_\mathrm{max} = 6 \Delta x

Number: 17 Author: zrick Subject: Cross-Out Date: 28.09.21, 15:09:57

Number: 18 Author: zrick Subject: Inserted Text Date: 28.09.21, 15:10:07

$L_z \ge 3 \delta$.

Number: 19 Author: zrick Subject: Cross-Out Date: 28.09.21, 15:09:56

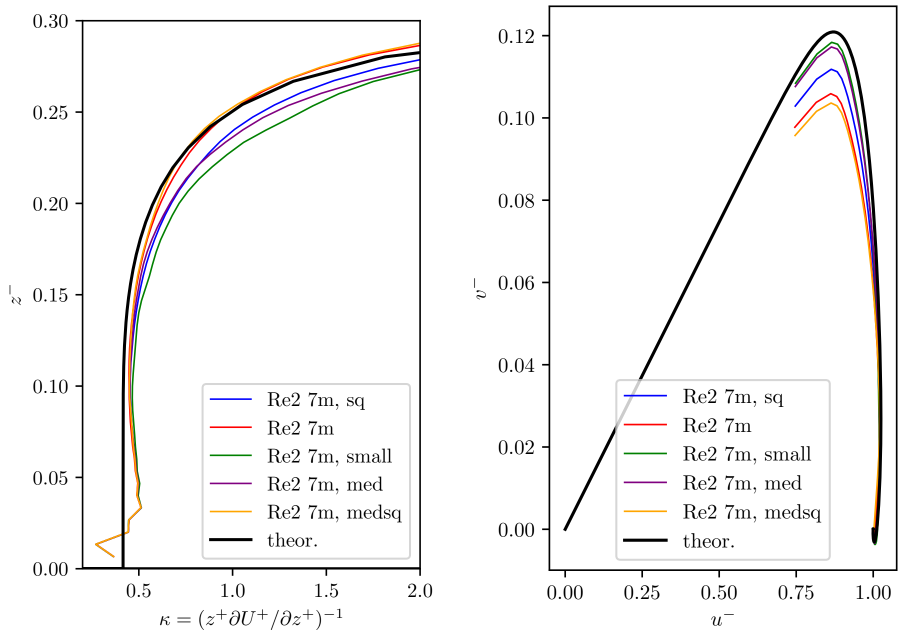

Figure 1: Left: $\kappa = d\log(z^+)/dU^+$. Right: hodograph.

simulation results...] In part I of this publication, the DNS of low Reynolds number simulations ($Re_D \leq 1\,600$) have a horizontal domain length of $L_x = 0.54\Lambda_{Ro}$ or $L_x = 1.08\Lambda_{Ro}$, where $\Lambda_{Ro} = G/f$ is the Rossby radius. ~~([reason? include wavelengths that influence the profiles? citations?]).~~ For these Reynolds numbers, $u_\star/G$ is around 0.05 so $L_x = 0.54G/f \approx 10u_\star/f = 10\delta$ ([introduce δ_{95} as boundary layer height?]). However, $u_\star/G$ decreases with increasing Reynolds number and is around 0.02 for $Re_D = 10^6$. A domain size of half the Rossby radius would then extend to $L_x \approx 25\delta$. Such a large domain would imply immense computational costs. To avoid this, the horizontal domain length was chosen to be $L_x \approx 10\delta$ for all Reynolds numbers, which is $L_x/(G/f) \approx 0.48, 0.25, 0.22$ for $Re1$, $Re2$, and $Re3$, respectively. An overview over the parameters of the settings is presented in table 2. [Cite other domain sizes: Jiang et al. [2018] test domain size of 512x512 grid points or 2048x2048m, which means $L_x \approx 0.04\Lambda_{Ro}$, normal domain only half of this size: $L_x \approx 0.02\Lambda_{Ro}$. Spalart et al. [2008] $\Lambda_x = 2u_\star/f$, justified by Csanady [1967] ("... it determines the size of the largest outer-layer eddies."). Esau [2004] $L_x = 0.08\Lambda_{Ro}$.]

~~As LES uses a much coarser resolution than DNS, unresolved processes like~~ the turbulent transport on the subgrid scale need to be modeled by a subgrid-scale model (SGS model). The model code of PALM offers two different SGS models: a 1.5-order closure after Deardorff [1980] and a dynamic closure after Heinz [2008]. For most of the simulations, the 1.5-order closure is used, but several simulations are repeated using the dynamic closure for comparison.

The problem is solved using a three-step Runge-Kutta method. For scalar advection a 5th order Wicker-Skamarock scheme is employed. A comprehensive description of the LES model is given by Maronga et al. [2020a].

3.2 Correction of Mean Velocity

The initial profile of the flow is calculated by a 1d-model with a Reynolds-average based turbulence parametrization. At the beginning of the ~~3d~~, random perturbations are imposed ~~to~~ the horizontal velocity field to trigger the evolution of turbulent eddies. The following imbalance between pressure force and Coriolis force results in an inertial oscillation of the period

Number: 1 Author: zrick Subject: Inserted Text Date: 28.09.21, 15:14:24

The reason is simply that we do not know u* a priori, so we have to prescribe the domain size in terms of either G/f or in terms of D. The beauty of using Λ is that it does not depend on Re, so it is constant across cases. D increases with the square root of viscosity, so it would attain a different numerical value for each Re.

Number: 2 Author: zrick Subject: Highlight Date: 28.09.21, 15:28:15

definitely very nice idea. In particular: DOI 10.1007/s10546-014-9950-2 (Shah and Bou-Zeid, BLM 2014 and references on their second page (p.357)

Number: 3 Author: zrick Subject: Cross-Out Date: 28.09.21, 15:28:54

Number: 4 Author: zrick Subject: Inserted Text Date: 28.09.21, 15:28:58

In LES,

Number: 5 Author: zrick Subject: Inserted Text Date: 28.09.21, 15:32:48

* [insert PALM reference from below here]

Number: 6 Author: zrick Subject: Inserted Text Date: 28.09.21, 15:33:09

[no paragraph break here]

Number: 7 Author: zrick Subject: Inserted Text Date: 28.09.21, 15:30:02

3rd-order [???]

Number: 8 Author: zrick Subject: Inserted Text Date: 28.09.21, 15:30:14

low-storage [???]

Number: 9 Author: zrick Subject: Highlight Date: 28.09.21, 15:32:26

move reference to (*) above

Number: 10 Author: zrick Subject: Inserted Text Date: 28.09.21, 15:30:38

- [add dash]

Number: 11 Author: zrick Subject: Cross-Out Date: 28.09.21, 15:38:09

Number: 12 Author: zrick Subject: Inserted Text Date: 28.09.21, 15:38:19

three-dimensional simulation

Number: 13 Author: zrick Subject: Inserted Text Date: 28.09.21, 15:37:00

on?

Number: 14 Author: zrick Subject: Cross-Out Date: 28.09.21, 15:38:42

Number: 15 Author: zrick Subject: Inserted Text Date: 28.09.21, 15:38:45

C

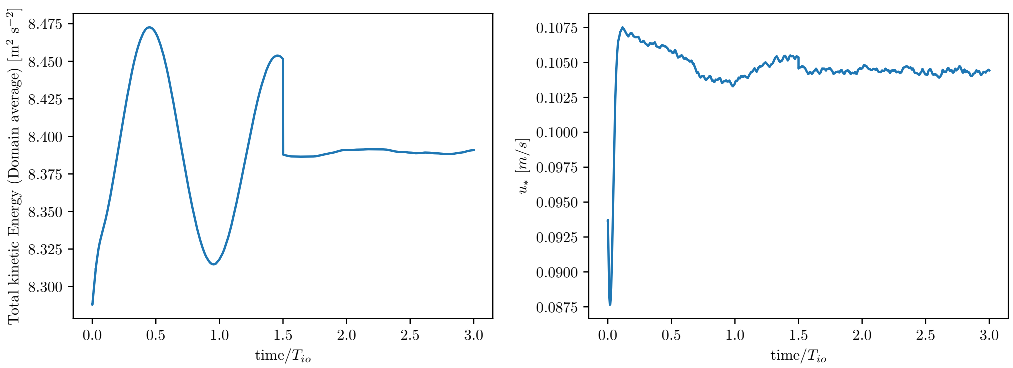

Figure 2: Left: domain-averaged kinetic energy of the simulation Re2_100. Right: horizontal average of the friction velocity

$T_{io} = 2\pi/f$. The oscillation slowly decays over time and eventually vanishes. To avoid an overly long spin-up time, an ensemble average of the horizontal wind profiles $\langle U\rangle(z)$ and $\langle V\rangle(z)$ is taken over a period of $T_{avg} = T_{io}$ after an evolution of turbulence for $T_{spin-up} = T_{io}/2$. At the point in time $t = \frac{3}{2}T_{io}$, the momentary wind field is adjusted such that the instantaneous domain-averaged wind profiles $\overline{U}(z)$ and $\overline{V}(z)$ are shifted to the values of the ensemble average over a whole inertial period:

$$u_{ijk}^{new} = u_{ijk} - \overline{U}_k + \langle U\rangle_k, \tag{15}$$

where i and j indicate the horizontal grid points and k indicates the vertical grid point. After this transformation of the flow field, the inertial oscillation is nearly gone and the simulation is continued for another period T_{io} to collect data for the evaluation. The effect of this correction of the mean velocity on the inertial oscillation is shown in fig. 2. This procedure seems to work better for low Reynolds numbers and for high Reynolds numbers simulated with coarse resolutions. This can be explained by the fact that the we only correct the mean velocity of the flow ~~and~~ while the form and orientation of the turbulent structures remains unchanged. Hence, after the correction, the mean velocity of both components corresponds the the mean of the the inertial period, whereas the ~~current eddies correspond to a still swinging flow before the correction.~~ So the structure and orientation of the turbulence is still off balance and might induce another inertial oscillation which is stronger for well resolved flows, since more turbulence is resolved. Nevertheless, through the procedure of correcting the mean profile after the recording over an inertial period we could remove the greater part of the inertial oscillation.

3.3 Choice of z_0

In contrast to DNS, the viscosity of the fluid hardly influences the flow on the grid scale of the LES, so the terms in the Navier-Stokes equation containing ν are neglected and only the Euler equations are solved. Instead of a no-slip condition at the bottom, a constant flux layer is assumed below the first grid point and the Monin–Obukhov theory is used to compute the friction velocity and the stresses at the first grid point:

$$u_\star = \frac{\kappa(U^2 + V^2)^{0.5}}{\ln{(z/z_0)}}, \tag{16}$$

$$-\overline{u''w''}_0 = \frac{\kappa U u_\star}{\ln{(z/z_0)}}. \tag{17}$$

Number: 1 Author: zrick Subject: Cross-Out Date: 28.09.21, 15:45:35

Number: 2 Author: zrick Subject: Inserted Text Date: 28.09.21, 15:45:31

,

Number: 3 Author: zrick Subject: Inserted Text Date: 28.09.21, 15:45:35

it would

Number: 4 Author: zrick Subject: Inserted Text Date: 28.09.21, 15:45:45

for the dissipative nature of the turbulent flow

Number: 5 Author: zrick Subject: Highlight Date: 28.09.21, 15:49:26

isn't it quite uncommon to use angle brackets for the time average and an overbar for the horizontal average? Also: in a strict sense, both are ensemble averages, so it might be a little more clear to talk about time and space averaging. At least, these two would need the overbar too unless you define the angle bracket to include the overbar... Else, equation 15 appears to differentiate between two kinds of averaging, which it does not.

Number: 6 Author: zrick Subject: Highlight Date: 28.09.21, 15:52:56

would it be possible to illustrate this by adding two more curves or so to Figure 2? You would probably have to plot the normalized deviation of TKE where you normalize by either the final value or the all-time average.

Number: 7 Author: zrick Subject: Cross-Out Date: 28.09.21, 15:50:24

Number: 8 Author: zrick Subject: Inserted Text Date: 28.09.21, 15:54:15

turbulent spectrum at wavenumbers other than zero carries forth the memory of the inertial oscillation.

Number: 9 Author: zrick Subject: Cross-Out Date: 28.09.21, 15:54:27

Number: 10 Author: zrick Subject: Inserted Text Date: 28.09.21, 15:54:33

, however, much smaller,

Number: 11 Author: zrick Subject: Inserted Text Date: 28.09.21, 15:55:58

For the linear character of the inertial oscillation, these higher-order effects (i.e. those ones not carried in the mean of the flow) are, however, small, and the procedure reduce the magnitude of the inertial oscillation by approximately one order of magnitude.

Number: 12 Author: zrick Subject: Highlight Date: 28.09.21, 16:14:01

Given that the paper is really quite explicitly comparing DNS and LES, I would use a couple of more sentences here and suggest to be very clear and careful:

"In LES, one postulates that a sufficient part of the largest eddies (from a spectral perspective) is resolved so as to represent the non-linear effects of turbulent mixing. Below these resolved scales, turbulence is modelled as a more or less isotropically acting diffusive agent through a closure model (Dynamic, Smagorinsky, RANS, see above). Consequently, molecular friction is not considered directly, but only by virtue of a turbulence model that links the resolved scales and the dissipative scales. In their seminal works on the spectral energy transfer in homogeneous isotropic turbulence, Kolmogorov and Obukhov (1941, 1942) showed that the rate of energy transfer across the spectrum is in fact a constant implying that the rate of transfer across the cut-off scale in LES does not depend on the magnitude of the viscous scale, presupposed that (i) the cut-off scale of the LES is well within the inertial range and (ii) that the LES turbulence is approximately isotropic and homogeneous at the smalles resolved scales. This implies that an LES turbulence closure need not carry explicit information on the Reynolds number or viscosity of the flow.

In contrast to the interior closure of the LES where one can drop the dissipative effects entirely, this is not possible for the viscid effects related to roughness which act in immediate vicinity to the surface. Here, instead of a no-slip condition .... [continue as in manuscript]"

[and now that it's written, this has, not much to do with z_0 and should probably go either into the introduction or the LES description, but in my opinion, it is very important]

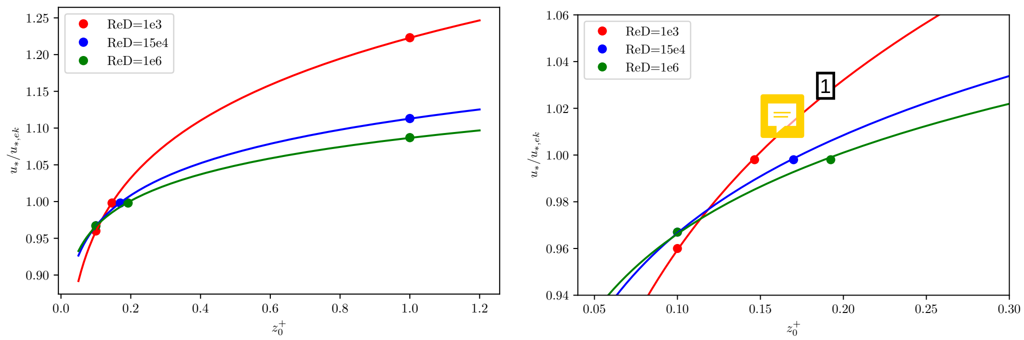

Figure 3: The friction velocity as function of the roughness length with fit

Nevertheless, the viscosity is taken into account indirectly by choosing the roughness length z_0. ~~This becomes clear by~~ considering the law of the wall for a smooth surface:

$$u^+ = \frac{1}{\kappa}\ln(z^+) + C^+ = \frac{1}{\kappa}\ln\left(\frac{z^+}{z_0^+}\right) \tag{18}$$

with $\kappa \approx 0.416$ and $C^+ \approx 5.4605$ for a smooth wall (reference?). This leads to

$$z_0^+ = \exp\left(-\kappa C^+\right) \approx \cancel{0.1} \tag{19}$$

which is the roughness length for a smooth wall in inner units. ~~So~~ the roughness length in SI-units $z_0 = z_0^+\nu/u_\star \approx 0.1\nu/u_\star$ depends on the viscosity of the fluid, which means that the choice of z_0 ~~is equivalent ([?]) to a choice of the~~ viscosity ν.

The choice of z_0 and ~~the turbulent flow (driven by~~ the geostrophic wind G) determine the magnitude of $u_\star$ in a non trivial way. As will be demonstrated below, the choice of $z_0 = 0.1$ does not lead to the ~~expected~~ value of $u_\star$ predicted by Spalart. To reproduce the predicted $u_{\star pred}$, a sensitivity study was performed whose results are shown in fig. 3. A variation of z_0^+ showed that the resulting $u_\star$ follow a power law $u_\star/u_{\star pred} = a(z_0^+)^m$. In order to get the expected friction velocity, z_0^+ had to be 0.149, 0.174, and 0.196 for the cases Re1, Re2, and Re3, respectively. As these are the values for Reynolds numbers that differ by three orders of magnitude, this is only a slight dependence on the Reynolds number.

4 Results

The theoretical profiles of both horizontal velocity components as well as corresponding LES solutions for all three Reynolds numbers are shown in fig. 4. At first sight, the similar form of the profiles for all Reynolds numbers is apparent. In the viscous sublayer, the shear-aligned component increases linearly up to the buffer layer around $z^+ \approx 19$, where it ~~(übergehen)~~ slowly into the logarithmic layer. There the ~~U-~~component increases logarithmically up to the supergeostrophic maximum and above decreases to its geostrophic value. The V-component plays nearly no role up to the middle of the logarithmic layer, where the transition to the Ekman layer takes place ($z^- \approx \cancel{0.3} - \cancel{120/Re_D}$). In inner scaling, the V-component of all Reynolds numbers is very similar, while the growth of the U-component leads to a smaller angle α for higher Reynolds numbers. In outer scaling, the profiles of the shear-aligned velocity deficit collapse in the upper part of the boundary layer and the profiles of the V-component's velocity deficit collapse for the whole boundary layer.

The length of the profiles from the LES is identical for all Reynolds numbers. This is due to the fact that for all simulations, the ratio between boundary layer height and grid size is

Page: 7

Number: 1 Author: zrick Subject: Sticky Note Date: 28.09.21, 16:35:17

I don't think, we need this zoom-panel; if anything, it might be added to the right panel. Alternatively, eq. 18 gives perfect justification to use a log scale for z0^+ (or maybe even an inverse log, i.e. ln(1/z0^+)

Number: 2 Author: zrick Subject: Cross-Out Date: 28.09.21, 16:15:14

Number: 3 Author: zrick Subject: Highlight Date: 28.09.21, 16:14:35

We immediately see that

Number: 4 Author: zrick Subject: Inserted Text Date: 28.09.21, 16:15:17

when

Number: 5 Author: zrick Subject: Cross-Out Date: 28.09.21, 16:15:04

Number: 6 Author: zrick Subject: Highlight Date: 28.09.21, 16:16:07

I don't think, you need to give the values here. For that particular choice, you can just refer to part 1.

Number: 7 Author: zrick Subject: Inserted Text Date: 28.09.21, 16:36:16

, and for an aerodynamically smooth flow, this coefficient is on the order of 0.1.

Number: 8 Author: zrick Subject: Cross-Out Date: 28.09.21, 16:16:24

Number: 9 Author: zrick Subject: Inserted Text Date: 28.09.21, 16:16:26

T

Number: 10 Author: zrick Subject: Inserted Text Date: 28.09.21, 16:16:31

hence

Number: 11 Author: zrick Subject: Cross-Out Date: 28.09.21, 16:17:09

Number: 12 Author: zrick Subject: Inserted Text Date: 28.09.21, 16:18:14

; we, however, note that this approach combines the great uncertainties in specifying the roughness parameter with the scale separation. [Is this clear to you? IF not, we have to discuss and add a little more explanation]

Number: 13 Author: zrick Subject: Inserted Text Date: 28.09.21, 16:17:05

implies a particular value for

Number: 14 Author: zrick Subject: Cross-Out Date: 28.09.21, 16:18:43

Number: 15 Author: zrick Subject: Cross-Out Date: 28.09.21, 16:18:46

Number: 16 Author: zrick Subject: Inserted Text Date: 28.09.21, 16:18:56

s

Number: 17 Author: zrick Subject: Cross-Out Date: 28.09.21, 16:24:21

Number: 18 Author: zrick Subject: Inserted Text Date: 28.09.21, 16:24:43

semi-empirical considerations (cf. Spalart, 1989)

Number: 19 Author: zrick Subject: Inserted Text Date: 28.09.21, 16:20:20

, similar to the dependence of u* on the Reynolds number (or even smaller [???])

Number: 20 Author: zrick Subject: Inserted Text Date: 28.09.21, 16:56:24

transitions

Number: 21 Author: zrick Subject: Inserted Text Date: 28.09.21, 16:56:31

,

Number: 22 Author: zrick Subject: Inserted Text Date: 28.09.21, 16:56:37

streamwise

Number: 23 Author: zrick Subject: Inserted Text Date: 28.09.21, 16:58:55

0.28 - \sqrt(5/Re_D)

Number: 24 Author: zrick Subject: Highlight Date: 28.09.21, 17:03:37

Comments from page 7 continued on next page

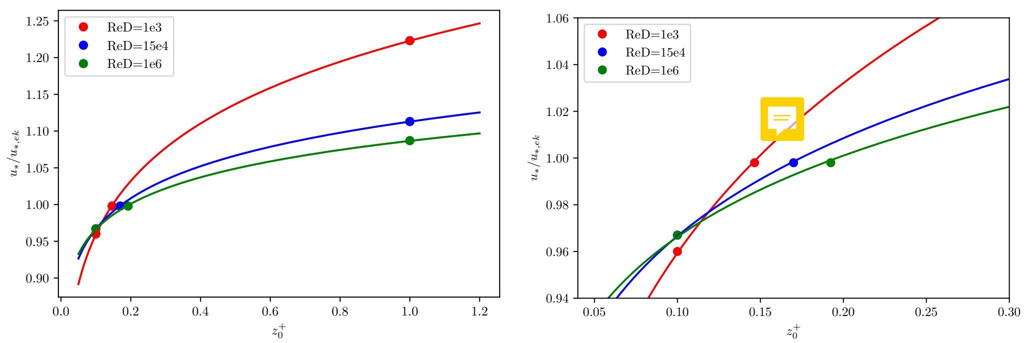

Figure 3: The friction velocity as function of the roughness length with fit

Nevertheless, the viscosity is taken into account indirectly by choosing the roughness length z_0~~.~~ ~~This becomes clear by~~ considering the law of the wall for a smooth surface:

$$u^+ = \frac{1}{\kappa}\ln(z^+) + C^+ = \frac{1}{\kappa}\ln\left(\frac{z^+}{z_0^+}\right) \tag{18}$$

with $\kappa \approx 0.416$ and $C^+ \approx 5.4605$ for a smooth wall (reference?). This leads to

$$z_0^+ = \exp\left(-\kappa C^+\right) \approx \cancel{0.1}, \tag{19}$$

which is the roughness length for a smooth wall in inner units. ~~So t~~he roughness length in SI-units $z_0 = z_0^+\nu/u_\star \approx 0.1\nu/u_\star$ depends on the viscosity of the fluid, which means that the choice of z_0 ~~is equivalent ([?]) to a choice of~~ the viscosity ν~~.~~

The choice of z_0 and ~~the turbulent flow (driven by~~ the geostrophic wind G~~)~~ determine the magnitude of $u_\star$ in a non trivial way. As will be demonstrated below, the choice of $z_0 = 0.1$ does not lead to the ~~expected~~ value of $u_\star$ predicted by Spalart. To reproduce the predicted $u_{\star pred}$, a sensitivity study was performed whose results are shown in fig. 3. A variation of z_0^+ showed that the resulting $u_\star$ follow a power law $u_\star/u_{\star pred} = a(z_0^+)^m$. In order to get the expected friction velocity, z_0^+ had to be 0.149, 0.174, and 0.196 for the cases Re1, Re2, and Re3, respectively. As these are the values for Reynolds numbers that differ by three orders of magnitude, this is only a slight dependence on the Reynolds number

4 Results

The theoretical profiles of both horizontal velocity components as well as corresponding LES solutions for all three Reynolds numbers are shown in fig. 4. At first sight, the similar form of the profiles for all Reynolds numbers is apparent. In the viscous sublayer, the shear-aligned component increases linearly up to the buffer layer around $z^+ \approx 19$, where it ~~(übergehen)~~ slowly into the logarithmic layer. There the ~~U-~~component increases logarithmically up to the supergeostrophic maximum and above decreases to its geostrophic value. The V-component plays nearly no role up to the middle of the logarithmic layer, where the transition to the Ekman layer takes place ($z^- \approx \cancel{0.3} \; \underline{-} \; \cancel{120/Re_D}$). In inner scaling, the V-component of all Reynolds numbers is very similar, while the growth of the U-component leads to a smaller angle α for higher Reynolds numbers. In outer scaling, the profiles of the shear-aligned velocity deficit collapse in the upper part of the boundary layer and the profiles of the V-component's velocity deficit collapse for the whole boundary layer.

The length of the profiles from the LES is identical for all Reynolds numbers. This is due to the fact that for all simulations, the ratio between boundary layer height and grid size is

This is interesting, and in the sense of scale-similarity, one might explicitly comment on the fact that this in some way a shift along both (i) the spectrum (ii) the height.

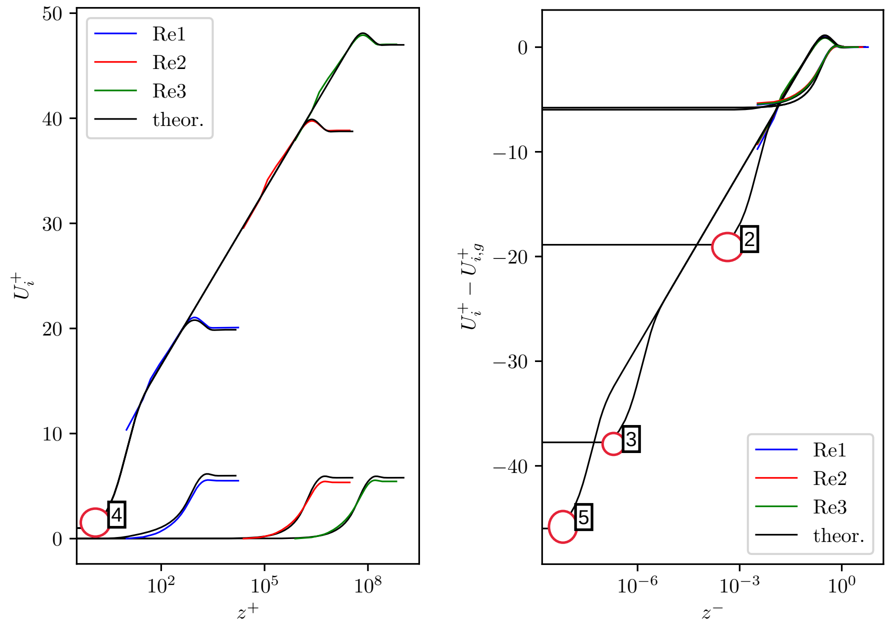

profiles are not correct below the red dots.

Figure 4: Left: shear-aligned profiles in outer scaling. Right: shear-aligned velocity deficit in inner scaling

similar, which leads to similar lengths from the first grid point to the boundary layer top in a logarithmic plot.

[Show dependence of the profiles of the domain size.]

The (expression?) $\kappa = d\log(z^+)/dU^+$ is quite sensitive to the resolution as well as to the domain size.

[Rating of the resolution as Jiang and Sullivan: value of κ, $z_{0,pr}$ estimated from profile vs. z_0, ΔW_{10}]

Estimation of κ: maximum height: where the value of $\kappa = d\log(z^+)/dU^+$ of the theoretical profile deviates by more than 2% of the used value $\kappa = 0.416$. minimum height: seventh grid point

The turbulent structures in boundary layers of high Reynolds numbers extend over a large range of scales. For the description of their vertical mean profiles, inner units ($z^+ = zu_*/\nu$, $U^+ = U/u_*$) and outer units ($z^- = z/\delta$, $U^- = U/G$) are used. At the lower boundary, the x-axis of the inner units is aligned with the shear stress, whereas the x-axis of the outer units is aligned with the geostrophic wind. The angle between both axes is called α.

A principal idea behind LES is to neglect the small scales of the flow and resolve only the large eddies, which carry most of the turbulent kinetic energy. Hence, the viscous sublayer and the buffer layer are not resolved by LES and cannot be compared. The first grid point of an LES usually lies inside of the logarithmic region of the boundary layer. Furthermore, the flow is usually underresolved in the lower layers of an LES, since near the bottom, the vertical component is massively restricted by the non-permeability of the wall.

δ_{95}: height where the turbulent stress decreased to 5% of its surface value. [put δ_{95}/δ in table. Which of both do we call boundary layer height?]

4.1 Logarithmic layer stream-wise velocity

[include $50 < z^+ < 0.15Re_\tau$, while $z^- = z^+Re_\tau$]

Figure 6 shows $\kappa = z^+\partial U^+/\partial z^+$, which is constant in the logarithmic layer. The theoretical profile shows a constant up to $z^- \approx 0.1$ for the case Re1 and up to $z^- \approx 0.15$ for the cases

Number: 1 Author: zrick Subject: Typewritten Text Date: 28.09.21, 17:01:03

profiles are not correct below the red dots.

Number: 2 Author: zrick Subject: Oval Date: 28.09.21, 17:00:24

Number: 3 Author: zrick Subject: Oval Date: 28.09.21, 17:00:31

Number: 4 Author: zrick Subject: Oval Date: 28.09.21, 17:01:08

Number: 5 Author: zrick Subject: Oval Date: 28.09.21, 17:00:36

Number: 6 Author: zrick Subject: Highlight Date: 28.09.21, 17:02:29

I would not bring this into Section 4 (either a subsection in 3 or an appendix). Here, I would try to argue that we use a sufficiently large case.

Number: 7 Author: zrick Subject: Inserted Text Date: 28.09.21, 17:06:03

; in fact -- irrespective of computational feasibility constraints -- this is also required for the MOST closure at the surface to remain valid(cf. Sec. 3.3).

Number: 8 Author: zrick Subject: Inserted Text Date: 28.09.21, 17:06:25

, known as blocking effect.

Number: 9 Author: zrick Subject: Highlight Date: 28.09.21, 17:06:52

definitely add to table. Introduce when introducing the nomenclature in Sec 2 or 3.

Number: 10 Author: zrick Subject: Highlight Date: 28.09.21, 17:08:54

the von K\'arm\'an measure, a constant in an idealized logarithmic layer

Number: 11 Author: zrick Subject: Inserted Text Date: 28.09.21, 17:09:06

near-

Number: 12 Author: zrick Subject: Inserted Text Date: 28.09.21, 17:09:12

value for

Table 3: Simulation results

Name	κ_{LES}	$z_{0,LES}/z_0$	δ_{95}/δ	$u_\star/u_{\star,dl}$	α/α_{dl} [°]
Re1_150	0.449	0.36	0.58	1.00	0.91
Re1_150_dyn	0.417	0.88	0.58	1.03	0.89
Re1_100	0.485	0.18	0.61	1.00	0.89
Re1_50	-	-	0.70	1.00	0.86
Re2_150	0.464	0.09	0.59	1.00	0.92
Re2_100	0.507	0.18	0.62	1.00	0.86
Re2_50	-	-	0.73	1.00	0.85
Re2_150_a	0.458	0.12	0.60	1.00	0.88
Re2_150_b	0.460	0.11	0.59	1.00	0.86
Re2_150_c	0.467	0.08	0.56	1.00	0.96
Re2_150_d	0.477	0.06	0.57	1.00	0.97
Re2_150_dyn	0.443	0.28	0.58	1.01	0.91
Re2_50_dyn	-	-	0.7	1.01	0.81
Re3_150	0.477	0.03	0.58	1.00	0.94
Re3_150_dyn	0.453	0.12	0.62	1.01	0.86
Re3_100	0.514	0.01	0.63	1.00	0.88
Re3_50	-	-	0.72	1.00	0.85

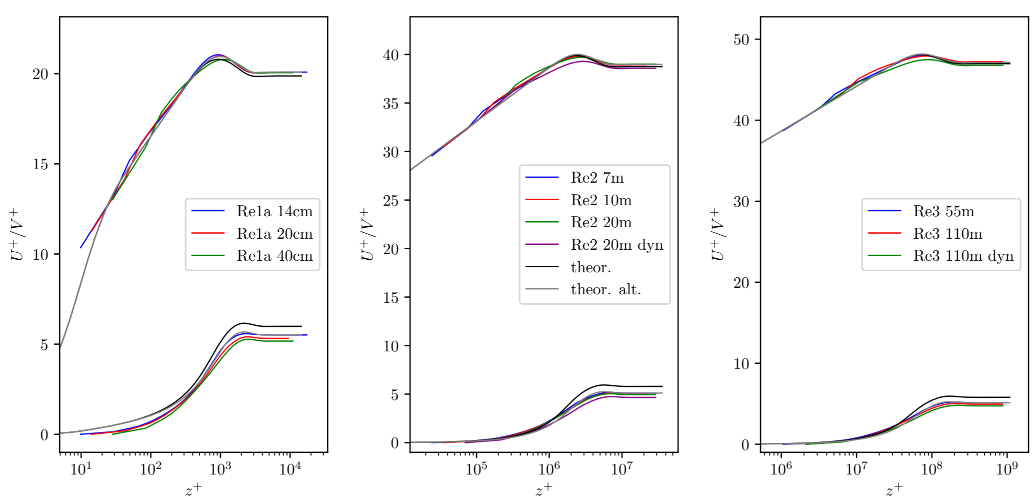

Figure 5: Shear-aligned profiles in inner scaling

This page contains no comments

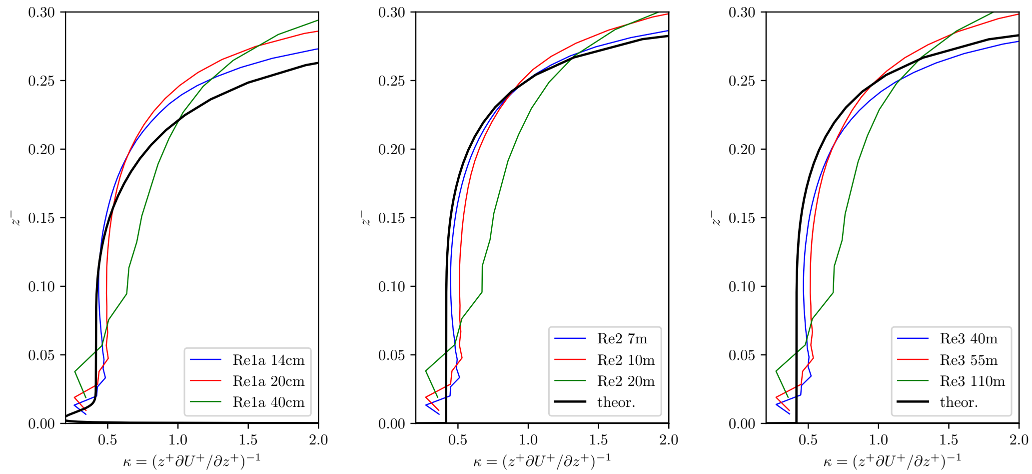

Figure 6: κ in the logarithmic region and above for different Reynolds numbers and resolutions

Re2 and Re3 [The logarithmic layer already begins to feel the outer layer] All cases have in common that an increase in resolution leads to a profile much closer to the theoretical curve.

A typical feature of LES is the log-layer mismatch of the first grid points above the bottom, comprehensively discussed by Brasseur and Wei [2010]. According to Maronga et al. [2020b], mean profiles follow MOST at height levels starting from the seventh grid above the surface. [[Jiang et al., 2018] identify an SGS-buffer layer which starts at ...] [define maximum deviation (in percent) from κ to define the height of the (nearly) purely logarithmic region. Between the seventh grid point and this height, κ of the LES is determined.]

An obvious feature of the low Reynolds number case is that the viscous sublayer represents a notable share of the boundary layer, while this layer is hardly visible for the high Reynolds number cases.

A Reynolds number of $Re_D = 1\,600$ is a very unusual Reynolds number for an LES. The first grid point of the LES lies at $\Delta/2$ and ~~should lie in the~~ logarithmic region of the boundary layer ~~(citation?)~~. For the finer resolved simulations of the low Reynolds number, the first grid point lies well in the buffer layer or even in the viscous sublayer. That means that the simulation results of this point are unlikely to produce reasonable results since an LES does not comprehend the physics needed to describe the behavior of the flow in this region.

The transition from buffer layer to logarithmic layer lies around $z^+ = 19$. The first grid point of the simulation *Re1* lies at $z^+ = 14$ for the 20 cm resolution and at $z^+ = 10$ for the 14 cm resolution.

The finest resolution ReX_150 resolves well the boundary layer in agreement with the findings of Wurps2019 where the neutral simulation was well resolved with more than 100 grid levels inside of the boundary layer δ_{95}. The ratio δ_{95}/δ is roughly 2/3 (slightly decreasing with Reynolds number). Hence, 150 grid levels within δ mean around 100 grid levels within δ_{95}.

4.2 Logarithmic layer span-wise velocity

Figure 8

4.3 Ekman layer

Hodograph: in reality (or DNS), the wind profile shows only a very little change of wind direction near the bottom, whereas LES starts ~~veering~~ from the first grid point on.

For the case Re1, the curves for all resolutions fall quite well onto the theoretical hodograph. For the cases Re2 and Re3, the hodographs clearly show that the veering is underestimated by

Page: 10

Number: 1 Author: zrick Subject: Inserted Text Date: 28.09.21, 17:11:38

'later' (higher up) for larger Re -- a consequence of the increased scale separation between inner and outer layer.

Number: 2 Author: zrick Subject: Sticky Note Date: 28.09.21, 17:12:31

Can we comment on what we or they think happens in between level 7 and the surface?

Number: 3 Author: zrick Subject: Inserted Text Date: 28.09.21, 17:13:13

For the staggering of vertical velocity,

Number: 4 Author: zrick Subject: Inserted Text Date: 28.09.21, 17:13:38

, as mentioned above, the surface-closure requires this to be contained within the

Number: 5 Author: zrick Subject: Cross-Out Date: 28.09.21, 17:13:44

Number: 6 Author: zrick Subject: Sticky Note Date: 28.09.21, 17:16:12

this is also important and interesting; we might extend. Can we possibly interpret this as simulating a surface which is smoother than aerodynamically smooth? (for sure, this is not possible in reality, but in a way a though experiment) What do you think?

Number: 7 Author: zrick Subject: Highlight Date: 28.09.21, 17:14:37

Number: 8 Author: zrick Subject: Highlight Date: 28.09.21, 17:15:22

correct curly braces.

Number: 9 Author: zrick Subject: Inserted Text Date: 28.09.21, 17:18:05

to veer

Number: 10 Author: zrick Subject: Inserted Text Date: 28.09.21, 17:17:59

--that does not explicitly resolve the viscous and buffer layer--

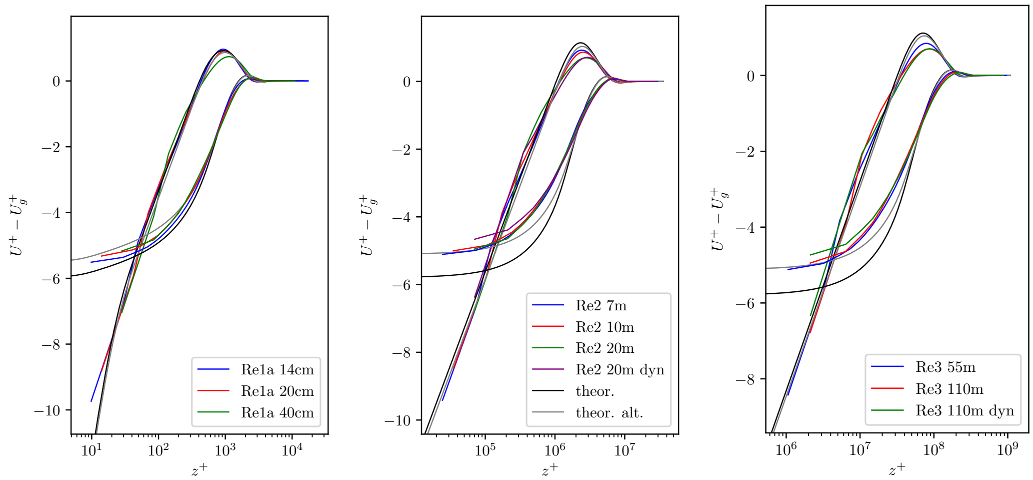

Figure 7: Shear-aligned velocity deficit

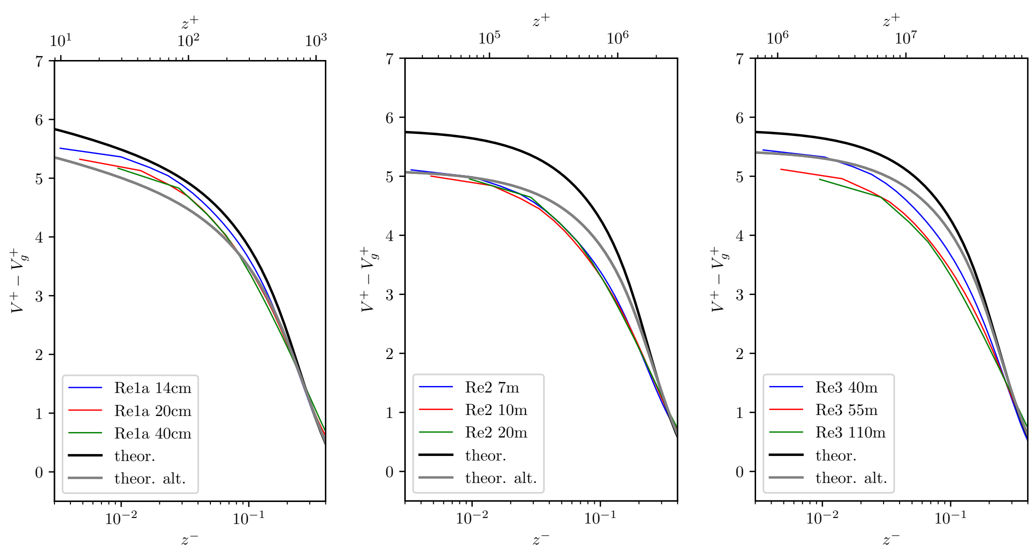

Figure 8: Shear-aligned velocity deficit of the v-component in the logarithmic layer

This page contains no comments

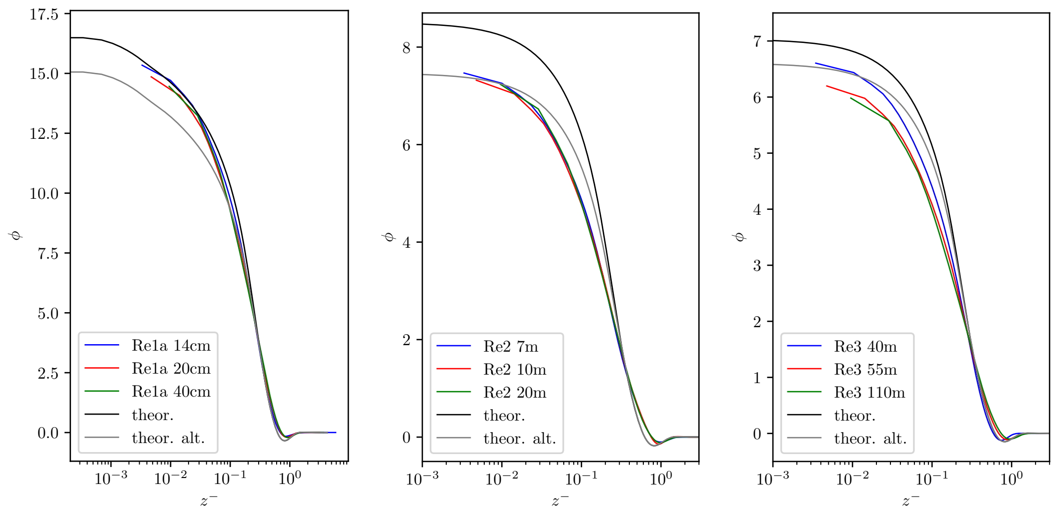

Figure 9: Direction of the mean flow with respect to the geostrophic wind.

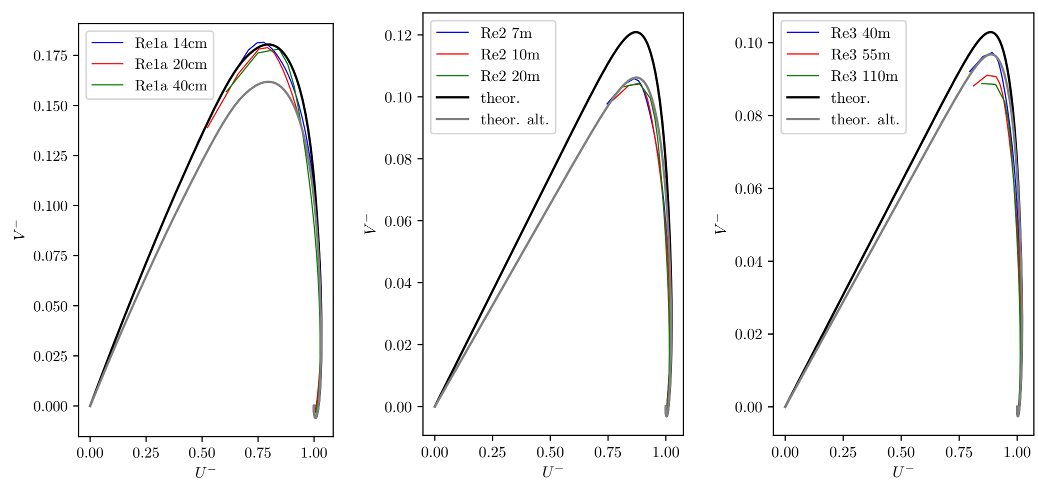

Figure 10: Geostrophy aligned hodograph

the LES.

There is a clear tendency that finer resolutions lead to a bigger α which is strongest for case Re3. Nevertheless, the predicted α is reached by non of the LES.

The adaption of the theoretical curve by using the α from the fines LES seems to be beneficial only for high Reynolds numbers. α is defined as the direction of the wind at the bottom while in LES we only have the direction of the wind at the first grid point: further veering below the first grid point is not taken into account. For high Reynolds numbers, the direction of the flow stays almost constant for a much wider part of the boundary layer (around 1% for Re2 and Re3), while for lower Reynolds number, the direction changes significantly much earlier (around 0.1% for Re1). The total α predicted by the theoretical profile (and the DNS) is 16.8° and the α of the LES with finest resolution of case Re1 is 15.3°. Despite this considerable difference, the curves match quite well and LES reproduces the correct course of wind directions at all heights above the first grid point.

Limits of coarse resolution - where is the MOST-Point in Hodograph?

Vergleich SGS-Modelle

As stated before, eq. 4 is very well validated for the range $400 < Re_D < 1\,600$ [Ansorge

This page contains no comments

and Mellado, 2014]. For Reynolds numbers like $Re_D = 1.5 \cdot 10^5$ or even $Re_D = 10^6$, there exist neither DNS nor experimental data. Hence, the solutions of eq. 4 are not to be taken as certainly correct and one might assume that the LES solution is not definitively incorrect. This being said, the theoretical profiles are recalculated with the values of $u_\star$ and α from the LES solution. [$u_\star$ genau messbar, G nicht. Trotzdem Spalart verlässlich? Integrale? Herleitung angucken. 1 Vielleicht ist Re für die LES anders? δ/z_0 Indeed, Jiang et al. [2018] use G, f and z_0 as input parameters – and these *are* the input parameters for an LES. Why are we adjusting z_0 to get the $u_\star$ predicted by Spalart [1989]?] 2 Simulations of Jiang et al. [2018] are not the same as ours, since their choice of z_0 is a real roughness length and not just caused by the viscosity and a flat plate. Their roughness lengths are so high that the resulting viscosity would have to be considered in the Navier-Stokes equations.

5 Discussion and Conclusions

Interesting comparison between DNS and LES

Overall: good fit between theoretical profile and LES

Resolution of LES matters a lot

Helpful for rating LES profile: height where profile should deviate from logarithmic shape.

Theoretical profiles provide a very detailed benchmark for all aspects of the flow. A very good hit of the hodograph might coincide with a poor curve for κ.

References

Cedrick Ansorge and Juan Pedro Mellado. Global intermittency and collapsing turbulence in the stratified planetary boundary layer. *Boundary-layer meteorology*, 153(1):89–116, 2014.

James G Brasseur and Tie Wei. Designing large-eddy simulation of the turbulent boundary layer to capture law-of-the-wall scaling. *Phys Fluids*, 22(2):021303, 2010.

GT Csanady. On the "resistance law" of a turbulent ekman layer. *Journal of Atmospheric Sciences*, 24(5):467–471, 1967.

James W Deardorff. Stratocumulus-capped mixed layers derived from a three-dimensional model. *Boundary-Layer Meteorology*, 18(4):495–527, 1980.

I Esau. Simulation of ekman boundary layers by large eddy model with dynamic mixed subfilter closure. *Environmental Fluid Mechanics*, 4(3):273–303, 2004.

Stefan Heinz. Realizability of dynamic subgrid-scale stress models via stochastic analysis. *Monte Carlo Methods Appl*, 14(4):311–329, 2008.

Qingfang Jiang, Shouping Wang, and Peter Sullivan. Large-eddy simulation study of log laws in a neutral ekman boundary layer. *Journal of the Atmospheric Sciences*, 75(6):1873–1889, 2018.

Björn Maronga, Sabine Banzhaf, Cornelia Burmeister, Thomas Esch, Renate Forkel, Dominik Fröhlich, Vladimir Fuka, Katrin Frieda Gehrke, Jan Geletič, Sebastian Giersch, et al. Overview of the palm model system 6.0. *Geoscientific Model Development*, 13(3):1335–1372, 2020a.

Björn Maronga, Christoph Knigge, and Siegfried Raasch. An improved surface boundary condition for large-eddy simulations based on monin–obukhov similarity theory: evaluation and consequences for grid convergence in neutral and stable conditions. *Boundary-Layer Meteorology*, 174(2):297–325, 2020b.

Page: 13

Number: 1 Author: zrick Subject: Highlight Date: 28.09.21, 17:21:35

Das ist m.E. der Hauptpunkt. Idealerweise würde das aber bedeuten, dass wir einen korrespndierenden mismatch in u* haben (hier erstmal nicht der Fall). Könnte man das aber evtl. durch ein anderes z_0 übereinanderbringen? Power-law ist ja bekannt...

Number: 2 Author: zrick Subject: Highlight Date: 28.09.21, 17:23:30

This is not clear to me. Explain better and let's talk about it next time.

Michael Optis, Adam Monahan, and Fred C Bosveld. Moving beyond monin–obukhov similarity theory in modelling wind-speed profiles in the lower atmospheric boundary layer under stable stratification. *Boundary-layer meteorology*, 153(3):497–514, 2014.

Philippe R Spalart. Theoretical and numerical study of a three-dimensional turbulent boundary layer. *Journal of Fluid Mechanics*, 205:319–340, 1989.

Philippe R Spalart, Gary N Coleman, and Roderick Johnstone. Direct numerical simulation of the ekman layer: A step in reynolds number, and cautious support for a log law with a shifted origin. *Physics of Fluids*, 20(10):101507, 2008.

H Tennekes. The logarithmic wind profile. *Journal of the Atmospheric Sciences*, 30(2):234–238, 1973.

This page contains no comments